Hindawi
International Journal of Corrosion
Volume 2018, Article ID 9696549, 10 pages
https://doi.org/10.1155/2018/9696549

Research Article

Anticorrosion Performance of LDH Coating Prepared by CO_2 Pressurization Method

Xiaochen Zhang,[1,2] **Peng Jiang**,[3] **Chunyan Zhang**,[4] **Bateer Buhe**,[2] **Bin Liu**,[1] **Yang Zhao**,[1] **Tao Zhang**,[4,5] **Guozhe Meng**,[1] **and Fuhui Wang**[5]

[1]*College of Materials Science and Chemical Engineering, Harbin Engineering University, Harbin 150001, China*
[2]*College of Materials Chemical and Engineering, Heilongjiang Institute of Technology, Harbin 150050, China*
[3]*School of Mechanical Engineering, Changzhou University, Changzhou 213164, China*
[4]*Institute of Metal Research, Chinese Academy of Sciences, Shenyang 110016, China*
[5]*School of Materials Science and Engineering, Northeastern University, Shenyang 110819, China*

Correspondence should be addressed to Tao Zhang; zhangtao@mail.neu.edu.cn

Received 22 May 2018; Revised 21 August 2018; Accepted 10 September 2018; Published 27 September 2018

Academic Editor: Ramazan Solmaz

Many surface treatment methods are used to improve the corrosion resistance of magnesium alloys. LDH (layered double hydroxides) conversion coatings are currently found in the most environmentally friendly and pollution-free coatings of magnesium alloy. In this study, the CO_2 pressurization method was applied to the preparation of LDH coating on magnesium alloy for the first time. The effect of CO_2 pressurization on the formation and corrosion resistance of LDH coating on AZ91D alloy was investigated. The hardness and adhesion were significantly higher on LDH coating in the case of CO_2 pressurization than it is in atmospheric pressure. The surface and cross-sectional morphologies show that LDH coating is more compact in the case of CO_2 pressurization than with atmospheric pressure. The results of the polarization curve, hydrogen evolution, and immersion tests indicate that the corrosion resistance of the LDH coating prepared by the CO_2 pressurization method was significantly improved.

1. Introduction

Magnesium and magnesium alloys are a "green engineering material" in the 21st century, having a wide range of application prospects, such as automotive, in aerospace, portable electronic devices, and in medicine. This is due to their superior strength-weight ratio, dimensional stability, light weight, recycling ability, and other excellent properties [1, 2]. However, the corrosion resistance of magnesium and magnesium alloys is extremely poor, severely restricting their further development [3, 4]. In order to expand the application of magnesium alloy and improve its corrosion resistance, the corrosion mechanism and surface protection of magnesium alloy materials have been studied extensively by domestic and foreign scholars [5–9]. Through surface modification and the coating on the surface of magnesium alloy, the defects of the corrosion resistance of magnesium alloys can be improved economically and effectively. Examples of this include conversion coating [10–12], anode oxidation [13, 14], electroplating [15, 16], and physical vapor deposition (PVD) [17, 18], among which the most widely used in the past decade is chromate conversion coating. Chromate conversion coating is a simple process, with the product coating demonstrating good heat stability and providing good protection for the magnesium alloy. However, chromate is toxic to the environment and hazardous to human beings, leading to it being banned in recent years. Lately, focus has turned to conversion coating that contains no chromium [12, 19, 20], such as phosphate [21, 22], phosphate-permanganate [23–25], stannate [26, 27], vanadate [28, 29], cerate [27, 30], lanthanite [31], and LDHs surface coatings [32–36]. Of these, LDH surface coating, as an environmentally friendly coating, has attracted more attention as it brings no pollution to the environment.

Layered double hydroxides (LDH) are environmentally friendly intercalation compounds. They are represented by

Table 1: Preparation parameters for three kinds of LDH conversion coatings.

Parameters	Temperature, ˚C	pH	Time, h	Pressure, MPa
1 [39, 40] CO_2_24h	50	4.3	24	0.1
2 [41–43] CO_2_2h/pH11.5_2h	50	4.3/11.5	4	0.1
3 CO_2_3MPa_0.5h	50	4.3	0.5	3

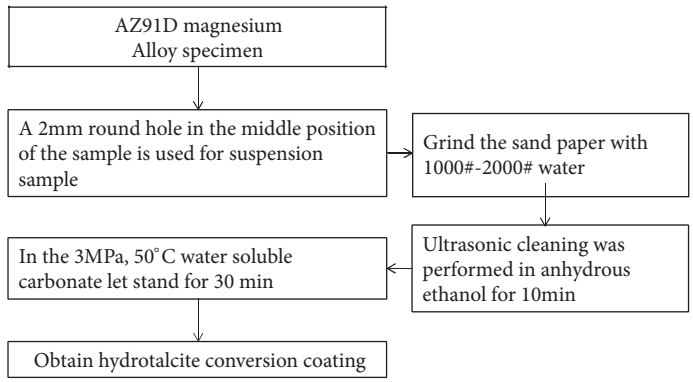

Figure 1: Operations for the preparation of conversion coating with CO_2 pressurization method.

a general formula of $[M_{1-x}^{2+}M_x^{3+}(OH)_2][A^{n-}]_{x/n}\cdot mH_2O$, where M^{2+} and M^{3+} represent divalent (e.g., Mg^{2+}, Ca^{2+}, Cu^{2+}, Mn^{2+}, Ni^{2+}, and Zn^{2+}) and trivalent metallic cations (e.g., Al^{3+}, Cr^{3+}, Fe^{3+}, Mn^{3+}, and Co^{3+}), respectively; X indicates the molar ratio of $M^{3+}/(M^{2+}+M^{3+})$ and its value ranges from 0.20 to 0.33, finally, with A^{n-} being an n^- valent anion, which is exchangeable anions. The anions (e.g., Cl^-, CO_3^{2-}, NO_3^-, and SO_4^{2-}) and variety of organic anions can be exchanged between the outside and interlayer spaces occupied by the water molecules [37, 38]. Uan et al. [39–43] proposed the characterization of Mg-Al hydrotalcite conversion coating on Mg alloy. Chen et al. [44–46] studied the in situ growth mechanism of Mg-Al hydrotalcite conversion coating on AZ31 magnesium alloy. Syu et al. [47] further studied an Li-Al-CO_3 double-phase hydroxide coating. Later, Zhang et al. [48] used a coprecipitation method to synthesize layered double hydroxides containing magnesium alloy. Wang et al. [49] synthesized hydrotalcite conversion coating on magnesium alloy.

In this study, considering the time consuming and weak antipollution properties owing to the complex process preparation of LDH conversion coatings for former process, a new method, CO_2 pressurization method, for preparing LDH conversion coatings was proposed. The introduction of a CO_2 pressurization method is based on the previous studies of Uan et al. [39–43]. LDH conversion coatings are prepared efficiently and quickly under CO_2 pressurization. A systematic investigation of the microstructure, hardness, adhesion, and corrosion resistance of LDH conversion coating is carried out.

2. Experiment

2.1. Material. For the purposes of this paper, AZ91D magnesium alloy was selected as the object material to be studied. It is composed of 8.8 wt.% Al, 0.69 wt.% Zn, 0.212 wt.% Mn, 0.02 wt.% Si, 0.002 wt.% Cu, 0.005 wt.% Fe, and 0.001 wt.% Ni. The AZ91D magnesium alloy ingot was cut into 20mm×12mm×6mm samples, each of which was ground with $1000^{\#}$-$2000^{\#}$-mesh SiC abrasive paper and ultrasonically cleaned in anhydrous ethanol.

2.2. Conversion Bath and Preparation of LDH Coating. All of the reagents/reactants used were clean and nonpolluting. In a typical preparation, the CO_2 was introduced in deionized water at room temperature with the flow rate of 1 dm^3/min for 20 min, in order to form the CO_3^{2-}/HCO_3^- solution. The pH of the bath was approximately 4.3 [39]. The LDH coating was prepared by means of three methods (see Table 1).

The first LDH coating was prepared by a one-step immersion method. The specimens were statically immersed in the bath at 50˚C for a particular period for 24h, denoted above as CO_2_24h treatment [39, 40]. The second LDH coating was prepared by a two-step immersion method. The specimens were immersed in the bath and CO_2 gas was continuously bubbled for 2h. Subsequently, the prep-treating bath was maintained at pH 11.5 by the dropwise addition of 1.25 M aqueous NaOH with vigorous stirring. The prep-treating specimens were immediately hydrothermally treated such treating at 50˚C for 2h. The two-step treatment was denoted as CO_2_2 h/pH11.5_2h [41–43]. The third LDH coating was prepared by the CO_2 pressurization method (see Figure 1). The bath was placed in an autoclave and then pressurized to 3MPa by pumping CO_2 gas, with the specimens of magnesium alloy being immersed in the autoclave at 50˚C and under for 0.5h. This was denoted above as CO_2_3MPa_0.5h.

2.3. Hardness and Adhesion. The HVS-5 digital Vickers hardness was used to test the Vickers hardness, with 5Kgf being loaded for 10s. The QFH type paint film was used to test the

Table 2: Adhesion test results of LDH conversion coatings with various processes.

Adhesions	Adhesion klass	Affected rate
1 CO_2_24h	1	<5%
2CO_2_2h/pH11.5_2h	1	<5%
3 CO_2_3MPa_0.5h	0	Almost never off

adhesion of the LDH coating, with the test results of the LDH coating being observed according to ISO2409-1974.

2.4. Microstructure. The surface and cross-sectional morphologies of LDH coating were observed by a Philips XL30 and JEOL JSM-6700F SEM, respectively. The microstructure was analyzed with X-ray diffraction (GAXRD) at Cu $k_{\alpha 1}$(1.5405 Å).

2.5. Corrosion Resistance. Potentiodynamic polarization measurements of AZ91D alloy with and without LDH coating were performed in an electrochemical workstation (Zennium, Zahner) with a three-electrode cell, using a platinum foil as the counter electrode and a saturated calomel electrode (SCE, saturated KCl) as the reference electrode in aerated 3.5wt% NaCl solution. The corrosion of magnesium alloy is mainly shown as the hydrogen evolution of the cathode. In order to avoid the influence of the cathode process on the whole electrochemical testing process, the anodic and cathodic polarization curves of the specimens were measured from the open circuit potential (OCP) to the anodic and cathodic side in the 300mv range, with a scan rate of 0.333mV·s^{-1}, respectively. The above measurements were repeated at least five times. Hydrogen evolution data were measured by collecting hydrogen from the reaction in a hydrogen collector. The samples were placed in a beaker containing 3.5wt% NaCl solution and in a water bath pot with a constant temperature (30±1°C). The burette was connected to the funnel, inverted into the solution, perpendicular to the sample to be tested, with it being noted that the top of the burette should be fully immersed in the solution. The hydrogen bubble produced by the magnesium alloy corrosion was introduced into the burette through the funnel so that the hydrogen evolution rate of the magnesium alloy and the film could be determined by the change of the reading on the burette after the hydrogen is collected. All of the hydrogen measurements were repeated at least three times. The immersion test was conducted to determine the corrosion rate of the AZ91D alloy with different LDH coating for 120 hours, with the macroscopic corrosion morphologies being obtained using a digital camera. For the immersion test, all measurements were repeated at least three times at 30 ± 1°C.

3. Results and Discussion

3.1. Effect of CO_2 Pressurization on Hardness and Adhesion. The effect of the CO_2 pressurization method on the hardness of the magnesium alloy surface is shown in Figure 2.

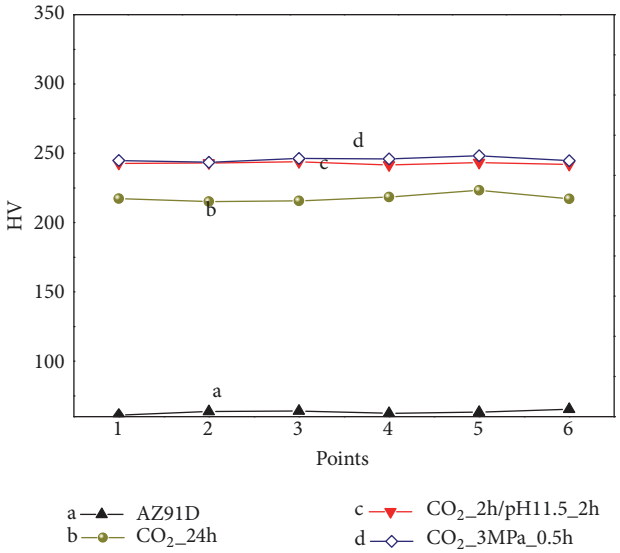

Figure 2: Hardness test results of the AZ91D alloy with and without LDH conversion coating.

The surface hardness was improved by the surface treatment and the hardness increased even more of the CO_2_3MPa_0.5h LDH coating. The macroscopic morphologies of the three specimens with different surface treatments after adhesion test are shown in Figure 3, where it can be clearly seen that the LDH coating detachment from the surface of the specimens was a mixed adhesive/cohesive fracture.

The results of the adhesion test are shown in Table 2). The cross cut tests are used to evaluate the adhesion of the conversion coating by attaching a 3M tape to the surface of the sample cross cut and removing it so as to observe the degree of detachment of the coating layer from the substrate. For the CO_2_2h/pH11.5_2h and CO_2_24h coating samples, the peeling area of the conversion film was less than 5%. The coating sample of CO_2_3MPa_0.5h showed almost never anything off of it. This suggests that the adhesion values can be ranked in the following descending order: CO_2_3MPa_0.5h > CO_2_24h ≈ CO_2_2h/pH11.5_2h.

3.2. Effect of CO_2 Pressurization on Microstructure. The surface and cross-sectional morphologies of LDH coating are shown in Figures 4 and 5. The surface morphology of the CO_2_3MPa_0.5h LDH coating was completely different from those of CO_2_24h and CO_2_2h/pH11.5_2h. The microcracks on the coating surface of CO_2_3MPa_0.5h almost disappeared, resulting in a dense and flat surface with island-like

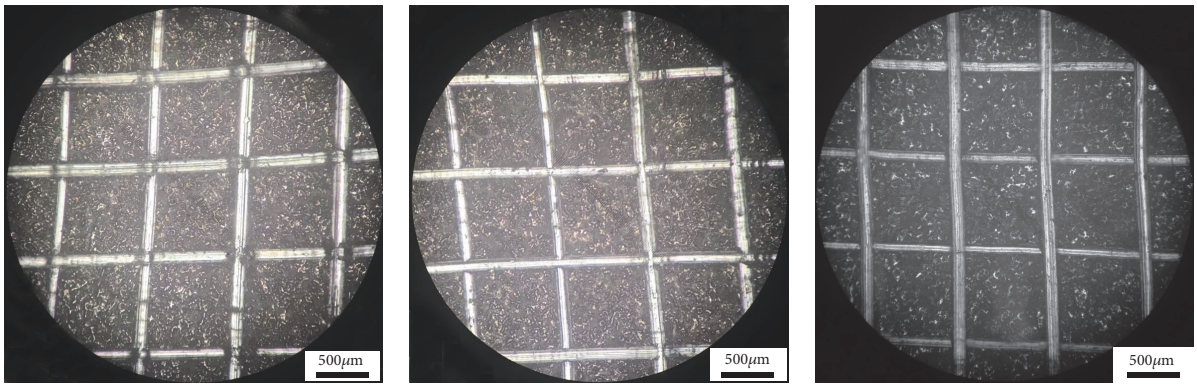

(a) (b) (c)

Figure 3: Adhesion test of conversion coatings with various process on AZ91D alloys: (a) CO_2_24h, (b) CO_2_2h/pH11.5_2h, and (c) CO_2_3MPa_0.5h.

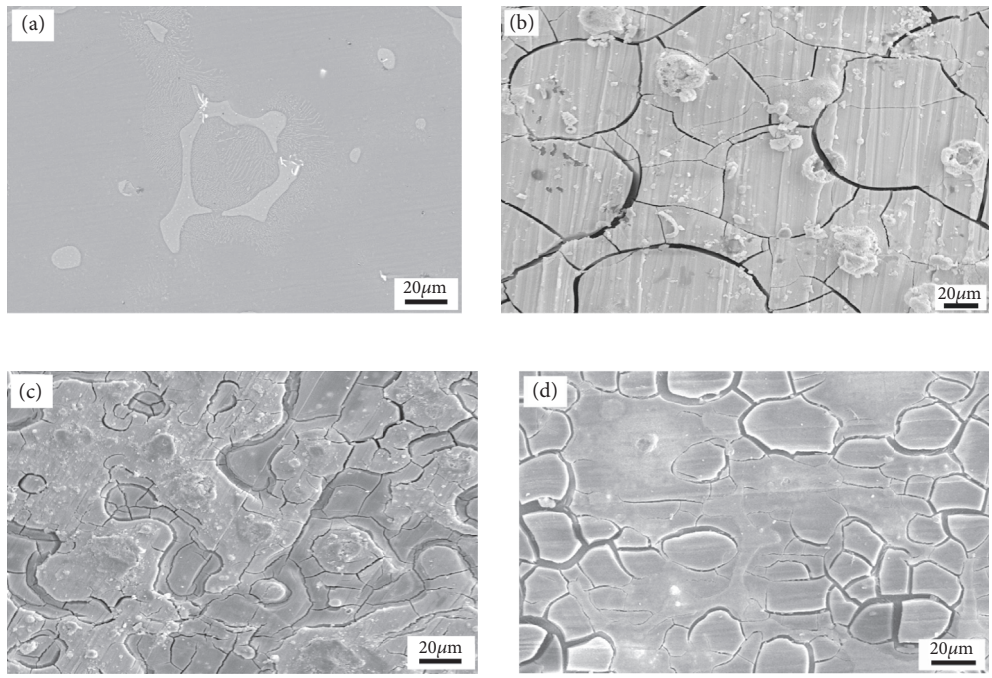

Figure 4: Morphologies of conversion coatings with various processes on AZ91D alloys: (a) unhandled-AZ91D, (b) CO_2_24h, (c) CO_2_2h/pH11.5_2h, and (d) CO_2_3MPa_0.5h.

features. Moreover, the cross-sectional morphology observation indicates that the CO_2_3MPa_0.5h LDH coating is compact, integral, and with less microcracks.

Opposed to this, CO_2_24h and CO_2_2h/pH11.5_2h show a large number of microcracks on the LDH coating, with the possibility that there are some cracks reaching the interface between the coating and the substrate.

The XRD patterns of the cast and different conversion coatings of AZ91D alloy are shown in Figure 6. The diffraction peaks of α-Mg, $Mg_{17}Al_{12}$, and LDH were detected. There were no discrepancies in the crystallographic orientations, with the diffraction peaks of LDH between the CO_2_24h, CO_2_2h/pH11.5_2h, and CO_2_3Mpa_0.5h specimens. However, there were higher peaks of LDH on the CO_2_3Mpa_0.5h specimen, indicating that the CO_2 pressurization method is easier for promoting the dynamic crystallization process of LDH conversion film on AZ91D magnesium alloy surfaces.

3.3. Effect of CO_2 Pressurization on Corrosion Resistance. The potentiodynamic polarization curves of the AZ91D alloy with and without conversion coatings are shown in Figure 7.

The corresponding electrochemical parameters, including corrosion potential (E_{corr}), corrosion current density (i_{corr}), and percentage of efficiencies (efficiency%), are calculated from the curves and listed in Table 3.

The hydrogen evolution rate (HER) of the AZ91D alloy with and without conversion coating is shown in Figure 8.

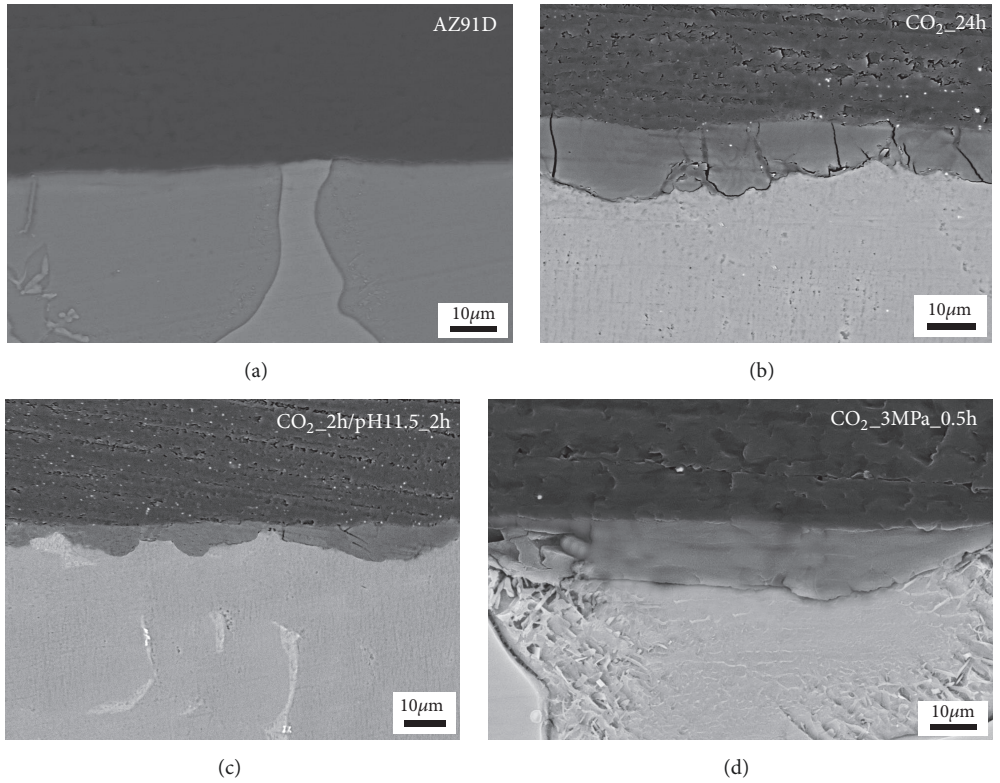

Figure 5: Cross-sectional microstructures of conversion coatings with various processes on AZ91D alloys: (a) unhandled-AZ91D, (b) CO_2_24h, (c) CO_2_2h/pH11.5_2h, and (d) CO_2_3MPa_0.5h.

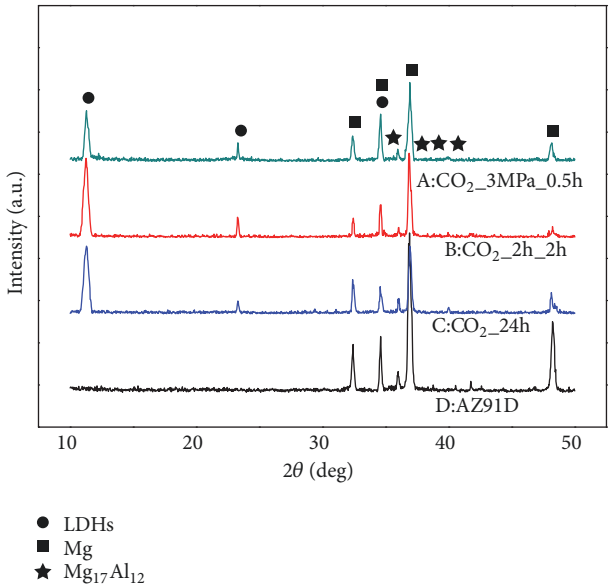

Figure 6: GAXRD patterns of the AZ91D alloy with and without conversion coating.

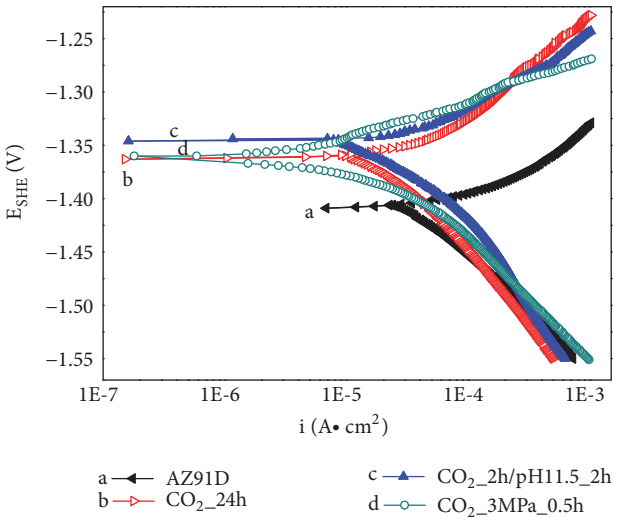

Figure 7: Polarization curves of the AZ91D alloy with and without conversion coating conversion coatings tested in 3.5wt.% NaCl solution.

It is well-known that the HER is proportional to the corrosion rate [48–52]. After the conversion treatment, the HER of CO_2_3MPa_0.5h coated AZ91D alloy (0.624±0.028 $mL \cdot h^{-1} \cdot cm^{-2}$) is lower by nearly 3 times that of the bare AZ91D alloy (1.920±0.114 $mL \cdot h^{-1} \cdot cm^{-2}$), implying that conversion coating improves the corrosion resistance of AZ91D alloy. Moreover, the HER of CO_2_3MPa_0.5h coating was approximately equal to that of the CO_2_2h/pH11.5_2h coating and lower than that of the CO_2_24h coating. An immersion

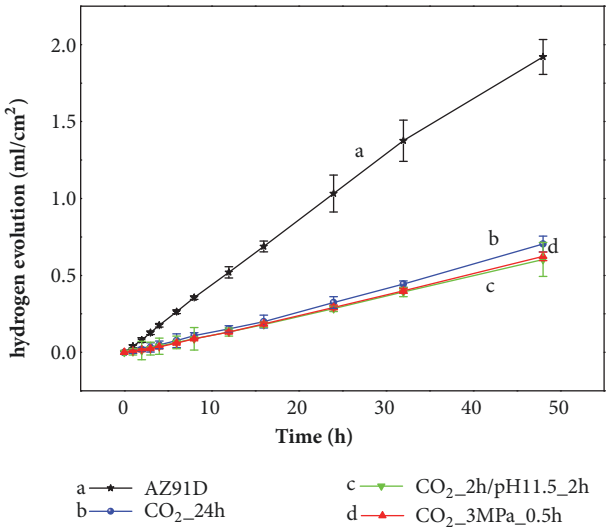

FIGURE 8: Hydrogen Evolution Curve of the AZ91D alloy with and without conversion coating in 0.6M NaCl solution.

test of 120 h was employed to evaluate the corrosion resistance of the conversion coatings. The macroscopic morphologies of AZ91D alloy with and without conversion coating are shown in Figure 9.

According to the Butler-Volmer equation, the corrosion current density (i_{corr}) should be determined based on the cathodic branch of the polarization curves by the Tafel extrapolation method [50], with i_{corr} being equal to the intersection of the horizontal line of the corrosion potential (E_{corr}) and the Tafel line of the cathodic process. It can be seen that the anodic reaction of AZ91D alloy is significantly inhibited. E_{corr} of the CO_2_3MPa_0.5h coating (-1.36 V) is higher than that of the AZ91D alloy (-1.41 V). Furthermore, i_{corr} of the coated AZ91D alloy (8.92±1.37 μA.cm^{-2}) is lower by nearly one order of magnitude than that of the bare AZ91D alloy (83.62±1.63 μA.cm^{-2}), indicating that the conversion coating effectively enhanced the corrosion resistance of the AZ91D alloy. Compared to the CO_2_24h and CO_2_2h/pH11.5_2h LDH coatings, the corrosion resistance of CO_2_3MPa_0.5h is also higher than the CO_2_24h and CO_2_2h/pH11.5_2h LDH coatings, embodying the lower i_{corr}. Moreover, the percentage of efficiencies (efficiency%), which is calculated from the ratio of i_{corr} with and without conversion coating, also shows that CO_2_3MPa_0.5h > CO_2_2h/pH11.5_2h > CO_2_24h. The above results show that i_{corr} of LDH coating can be ranked in the increasing series: CO_2_3MPa_0.5h < CO_2_2h/pH11.5_2h < CO_2_24h.

Additionally, the percentage of the surface area rusted for each specimen is estimated by using the visual examples according to ASTM D610-08. It is evident that the bare AZ91D alloy underwent severe attack rust grade 3G. Meanwhile, only several corroded spots are observed on the surfaces of the CO_2_3MPa_0.5h, CO_2_2h/pH11.5_2h, and CO_2_24h coated specimens, where the corresponding rust grades were 7G, 7G, and 6G, respectively. The results of the immersion test are in good agreement with those of the polarization curve and HER, indicating the improvement of the corrosion resistance of AZ91D alloy after CO_2_3MPa_0.5h conversion treatment.

According to the above results, the anticorrosion performance of LDH coating can be ranked in the following decreasing series: CO_2_3MPa_0.5h ≈ CO_2_2h/pH11.5_2h > CO_2_24h. However, the preparation efficiency of CO_2_3MPa_0.5h coating is 8 and 48 times higher than that of the CO_2_2h/pH11.5_2h and CO_2_24h coatings. Considering the corrosion resistance and preparation efficiency of the three coatings, the performance of CO_2_3MPa_0.5h coating is superior to that of the CO_2_2h/pH11.5_2h and CO_2_24h coatings.

3.4. Effect of CO_2 Pressurization on Film-Forming Power Process. The film-forming process of the LDH conversion coating is a kind of physical and chemical processes. The reaction process of the AZ91D magnesium alloy matrix material mainly includes an electrochemical reaction, an ionization reaction, and a coating-forming reaction in carbonate solution. Its specific chemical reaction equation is shown in formulae (1)~(6) [50–52].

$$Mg - 2e^- \longrightarrow Mg^{2+} \quad (1)$$

$$Al - 3e^- \longrightarrow Al^{3+} \quad (2)$$

$$2H^+ + 2e^- \longrightarrow H_2(g) \quad (3)$$

$$H_2CO_3 \longrightarrow HCO_3^- + H^+ \quad (4)$$

$$H_2CO_3 \longrightarrow CO_3^{2-} + 2H^+ \quad (5)$$

$$6Mg^{2+} + 2Al^{3+} + CO_3^{2-} + 16OH^- + 4H_2O \longrightarrow Mg_6Al_2(OH)_{16}CO_3 \cdot 4H_2O \quad (6)$$

The electrochemical reactions are shown in (1), (2), and (3), with it mainly being characterized as the dissolution of the metal of the anode and hydrogen ions of the cathode overflow. The ionization reactions are shown in (4) and (5), it basically being the ionization of the carbonate solution into the process of carbonate ions and bicarbonate ions. The film-forming reaction is shown in (6), with it mainly being the formation of a hydrotalcite conversion coating process, with magnesium ions, aluminium ions, carbonate ions, hydroxyl ions, and an aqueous solution. The vapor pressure of the solute in the dilute solution is proportional to the concentration of the solution, according to Henry's law. The higher the temperature, the smaller the solubility, the greater the pressure, and the greater the solubility at a certain temperature.

Due to the CO_2 pressurization, the CO_2 solubility in the solution increased, with the proportion of carbonate ions in the solution also increasing, resulting in an increase in the hydrogen ion concentration increased and promoting the electrochemical reaction to the right, thus accelerating the dissolution of the aluminium and magnesium ions. Further due to the CO_2 pressurization, the ionization is promoted to a positive reaction, accelerating, increasing the hydroxyl ions

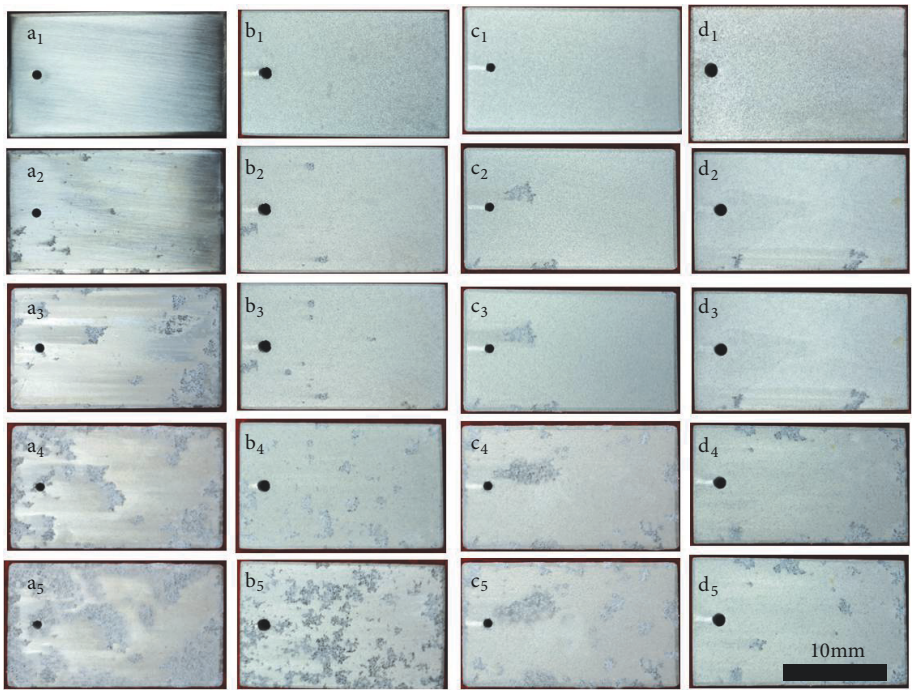

Figure 9: Optical corrosion morphologies of the AZ91D alloy with and without conversion coating of immersing test in 0.6M NaCl: (a_1) nonimmersed original sample, (a_2) original sample immersed for 24h, (a_3) original sample immersed for 48h, (a_4) original sample immersed for 72h, (a_5) original sample immersed for 120h, (b_1) nonimmersed CO_2_24h sample, (b_2) CO_2_24h sample immersed for 24h, (b_3) CO_2_24h sample immersed for 48h, (b_4) CO_2_24h sample immersed for 72h, (b_5) CO_2_24h sample immersed for 120h, (c_1) nonimmersed CO_2_2h /pH11.5_2h sample, (c_2) CO_2_2h/pH11.5_2h sample immersed for 24h, (c_3) CO_2_2h /pH11.5_2h sample immersed for 48h, (c_4) CO_2_2h /pH11.5_2h sample immersed for 72h, (c_5) CO_2_2h /pH11.5_2h sample immersed for 120h, (d_1) nonimmersed CO_2_3MPa_0.5h sample, (d_2) CO_2_3MPa_0.5h sample immersed for 24h, (d_3) CO_2_3MPa_0.5h sample immersed for 48h, (d_4) CO_2_3MPa_0.5h sample immersed for 72h, and (d_5) CO_2_3MPa_0.5h sample immersed for120h.

Table 3: Electrochemical test results of the AZ91D alloy with and without LDH conversion coating.

Samples	AZ91D	CO_2_2h/pH11.5_2h	CO_2_24h	CO_2_3Mpa_0.5h
E_{corr} (V, SCE)	1.41(±0.059)	-1.36(±0.026)	1.34(±0.054)	-1.36(±0.034)
i_{corr} (μA/cm^2)	83.62(±1.67)	15.81(±1.69)	17.34(±1.78)	8.92(±1.63)
efficiency%	-	81.1%	79.3%	89.3%

in the solution, and at the same time increasing the ionization reaction to the right, with the concentration of carbonate ion and bicarbonate ion in the solution being increased. The acceleration of the electrochemical reaction and ionization promoted the film-forming of the magnesium alloy matrix and the increase of the magnesium ions, aluminium ion, carbonate ions, and hydroxyl ions, promoting the film to a positive reaction and eventually improving the film-forming reaction rate. The film-forming process is shown in Figure 10.

In the initial stages, the conversion coating was very thin, with a small angular cavity or pit, such as a honeycomb cell, as can be seen in Figure 10(a). With the extension of the coating formation time, the conversion coating began to thicken and grow with layer, as shown in Figure 10(b). The surface was completely covered at 30 min, as show in Figure 10(c). With the cross-section of the coating, it can be found that the conversion coating first became in the α-Mg phase, with the conversion coating also present in the β-phase as the processing time increased. At 30 min, the surface of the magnesium alloy was covered with a complete and dense hydrotalcite conversion coating (see Figure 10).

4. Conclusion

The CO_2 pressurization method was first applied to the preparation of LDH coating on AZ91D alloy. The conversion coating first became in the α-Mg phase, with the conversion coating also present in the β-phase as the processing time increased. The formation rate of LDH coating was increased, indicating that the preparation efficiency can be improved greatly under CO_2 pressurization. Through this method, an LDH coating with higher thickness and less microcracks formed on the AZ91D alloy, significantly enhancing its anticorrosion performance. Compared to traditional processed, the anticorrosion performance of the CO_2_3MPa_0.5h coating was approximately equal to that of the CO_2_2h/pH11.5_2h

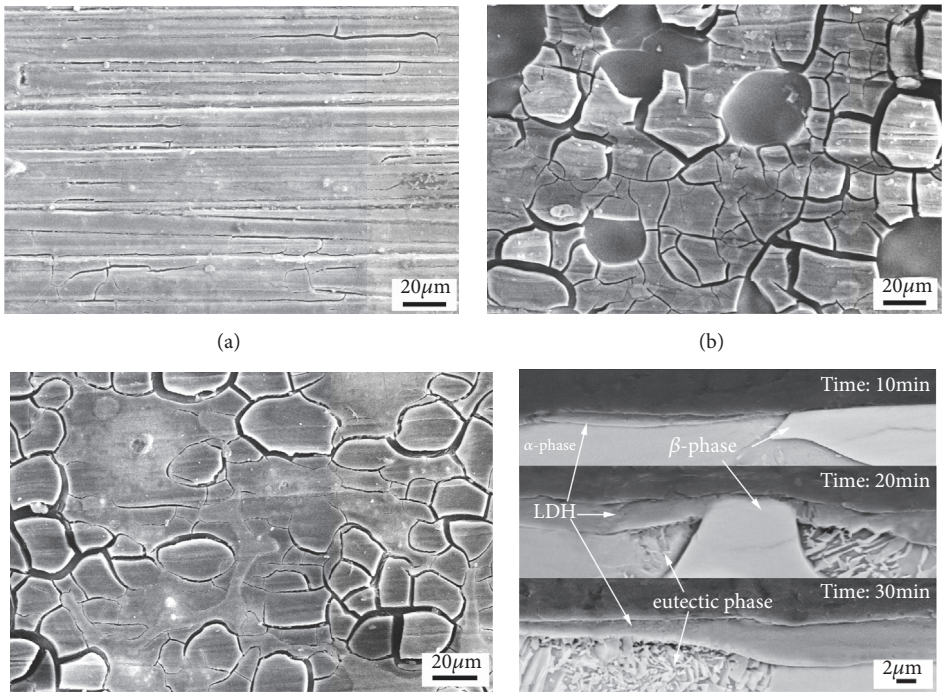

Figure 10: The film-forming process of the LDH conversion coating on the AZ91D magnesium alloy matrix material: (a) morphologies of the 10min sample, (b) morphologies of the 20min sample, (c) morphologies of the 30min sample, and (d) cross-sectional of conversion coating-forming process.

coating and was higher than that of the CO_2_24h coating. Considering the anticorrosion performance and preparation efficiency, the CO_2 pressurization method is a promising green technique for preparing LDH coating on magnesium alloy.

Data Availability

You can access the data through the link https://fairsharing.org/accounts/profile/.

Conflicts of Interest

The authors hereby declare that there are no conflicts of interest regarding the publication of this paper.

Acknowledgments

The authors wish to acknowledge the financial support of the National program for the Young Top-notch Professionals, the National Natural Science Foundation of China (nos. 51531007, 51771050, and 51705038), and Foundation of Young Scholars in HLJIT (2014QJ12).

References

[1] A. Atrens, G.-L. Song, M. Liu, Z. Shi, F. Cao, and M. S. Dargusch, "Review of recent developments in the field of magnesium corrosion," *Advanced Engineering Materials*, vol. 17, no. 4, pp. 400–453, 2015.

[2] Y. Zhao, L. Shi, X. Ji et al., "Corrosion resistance and antibacterial properties of polysiloxane modified layer-by-layer assembled self-healing coating on magnesium alloy," *Journal of Colloid and Interface Science*, vol. 526, pp. 43–50, 2018.

[3] F. Cao, G.-L. Song, and A. Atrens, "Corrosion and passivation of magnesium alloys," *Corrosion Science*, vol. 111, pp. 835–845, 2016.

[4] M. Esmaily, JE. Svensson et al., "Fundamentals and advances in magnesium alloy corrosion," *Prog. Mater. Sci*, vol. 89, pp. 92–193, 2017.

[5] M. Strzelecka, J. Iwaszko, M. Malik, and S. Tomczyński, "Surface modification of the AZ91 magnesium alloy," *Archives of Civil and Mechanical Engineering*, vol. 15, no. 4, pp. 854–861, 2015.

[6] Y. Su, Y. Guo, Z. Huang et al., "Preparation and corrosion behaviors of calcium phosphate conversion coating on magnesium alloy," *Surface and Coatings Technology*, vol. 307, pp. 99–108, 2016.

[7] Y. Gao, L. Zhao, X. Yao, R. Hang, X. Zhang, and B. Tang, "Corrosion behavior of porous ZrO 2 ceramic coating on AZ31B magnesium alloy," *Surface and Coatings Technology*, vol. 349, pp. 434–441, 2018.

[8] J. Yuan, R. Yuan, J. Wang et al., "Fabrication and corrosion resistance of phosphate/ZnO multilayer protective coating on magnesium alloy," *Surface and Coatings Technology*, vol. 352, pp. 74–83, 2018.

[9] X. Wang, L. Li, Z. Xie, and G. Yu, "Duplex coating combining layered double hydroxide and 8-quinolinol layers on Mg alloy

for corrosion protection," *Electrochimica Acta*, vol. 283, pp. 1845–1857, 2018.

[10] Z. Shao, Z. Cai, and J. Shi, "Preparation and Performance of Electroless Nickel on AZ91D Magnesium Alloy," *Materials and Manufacturing Processes*, vol. 31, no. 9, pp. 1238–1245, 2016.

[11] M. Esmaily, D. B. Blücher, J. E. Svensson, M. Halvarsson, and L. G. Johansson, "New insights into the corrosion of magnesium alloys—the role of aluminum," *Scripta Materialia*, vol. 115, pp. 91–95, 2016.

[12] R. Zeng, Y. Hu, F. Zhang et al., "Corrosion resistance of cerium-doped zinc calcium phosphate chemical conversion coatings on AZ31 magnesium alloy," *Transactions of Nonferrous Metals Society of China*, vol. 26, no. 2, pp. 472–483, 2016.

[13] G.-L. Song and Z. Shi, "Corrosion mechanism and evaluation of anodized magnesium alloys," *Corrosion Science*, vol. 85, pp. 126–140, 2014.

[14] A. F. Cipriano, J. Lin, C. Miller et al., "Anodization of magnesium for biomedical applications – Processing, characterization, degradation and cytocompatibility," *Acta Biomaterialia*, vol. 62, pp. 397–417, 2017.

[15] I. Saeki, T. Seguchi, Y. Kourakata, and Y. Hayashi, "Ni electroplating on AZ91D Mg alloy using alkaline citric acid bath," *Electrochimica Acta*, vol. 114, pp. 827–831, 2013.

[16] D. Yan, G. Yu, B. Hu, J. Zhang, Z. Song, and X. Zhang, "An innovative procedure of electroless nickel plating in fluoride-free bath used for AZ91D magnesium alloy," *Journal of Alloys and Compounds*, vol. 653, pp. 271–278, 2015.

[17] H. Altun and S. Sen, "The effect of PVD coatings on the wear behaviour of magnesium alloys," *Materials Characterization*, vol. 58, no. 10, pp. 917–921, 2007.

[18] H. Hoche, S. Groß, and M. Oechsner, "Development of new PVD coatings for magnesium alloys with improved corrosion properties," *Surface and Coatings Technology*, vol. 259, pp. 102–108, 2014.

[19] S. Pommiers, J. Frayret, A. Castetbon, and M. Potin-Gautier, "Alternative conversion coatings to chromate for the protection of magnesium alloys," *Corrosion Science*, vol. 84, pp. 135–146, 2014.

[20] X. Jiang, R. Guo, and S. Jiang, "Microstructure and corrosion resistance of Ce-V conversion coating on AZ31 magnesium alloy," *Applied Surface Science*, vol. 341, pp. 166–174, 2015.

[21] X.-B. Chen, H.-Y. Yang, T. B. Abbott, M. A. Easton, and N. Birbilis, "Corrosion protection of magnesium and its alloys by metal phosphate conversion coatings," *Surface Engineering*, vol. 30, no. 12, pp. 871–879, 2014.

[22] N. Van Phuong, M. Gupta, and S. Moon, "Enhanced corrosion performance of magnesium phosphate conversion coating on AZ31 magnesium alloy," *Transactions of Nonferrous Metals Society of China*, vol. 27, no. 5, pp. 1087–1095, 2017.

[23] S.-Y. Jian, Y.-R. Chu, and C.-S. Lin, "Permanganate conversion coating on AZ31 magnesium alloys with enhanced corrosion resistance," *Corrosion Science*, vol. 93, pp. 301–309, 2015.

[24] Y. L. Lee, Y. R. Chu, W. C. Li, and C. S. Lin, "Effect of permanganate concentration on the formation and properties of phosphate/permanganate conversion coating on AZ31 magnesium alloy," *Corrosion Science*, vol. 70, pp. 74–81, 2013.

[25] M. Mosiałek, G. Mordarski, P. Nowak et al., "Phosphate-permanganate conversion coatings on the AZ81 magnesium alloy: SEM, EIS and XPS studies," *Surface and Coatings Technology*, vol. 206, no. 1, pp. 51–62, 2011.

[26] L. Yang, M. Zhang, J. Li, X. Yu, and Z. Niu, "Stannate conversion coatings on Mg-8Li alloy," *Journal of Alloys and Compounds*, vol. 471, no. 1-2, pp. 197–200, 2009.

[27] Y. L. Lee, Y. R. Chu, F. J. Chen, and C. S. Lin, "Mechanism of the formation of stannate and cerium conversion coatings on AZ91D magnesium alloys," *Applied Surface Science*, vol. 276, pp. 578–585, 2013.

[28] Y. Ma, N. Li, D. Li, M. Zhang, and X. Huang, "Characteristics and corrosion studies of vanadate conversion coating formed on Mg-14 wt%Li-1 wt%Al-0.1 wt%Ce alloy," *Applied Surface Science*, vol. 261, pp. 59–67, 2012.

[29] L. Niu, S.-H. Chang, X. Tong, G. Li, and Z. Shi, "Analysis of characteristics of vanadate conversion coating on the surface of magnesium alloy," *Journal of Alloys and Compounds*, vol. 617, pp. 214–218, 2014.

[30] L. Lei, J. Shi, X. Wang, D. Liu, and H. Xu, "Microstructure and electrochemical behavior of cerium conversion coating modified with silane agent on magnesium substrates," *Applied Surface Science*, vol. 376, pp. 161–171, 2016.

[31] G. Kong, L. Liu, J. Lu, C. Che, and Z. ZHong, "Study on lanthanum salt conversion coating modified with citric acid on hot dip galvanized steel," *Journal of Rare Earths*, vol. 28, no. 3, pp. 461–465, 2010.

[32] N. Kamiyama, G. Panomsuwan, E. Yamamoto, T. Sudare, N. Saito, and T. Ishizaki, "Effect of treatment time in the Mg(OH)2/Mg–Al LDH composite film formed on Mg alloy AZ31 by steam coating on the corrosion resistance," *Surface and Coatings Technology*, vol. 286, pp. 172–177, 2016.

[33] Q. Dong, Z. Ba, and Y. Jia, "Efect of solution concentration on sealing treatment of Mg-Al hydrotalcite film on AZ91D Mg alloy," *J. Magnes. Alloy*, vol. 5, pp. 320–325, 2017.

[34] L. Guo, W. Wu, Y. Zhou, F. Zhang, R. Zeng, and J. Zeng, "Layered double hydroxide coatings on magnesium alloys: A review," *Journal of Materials Science and Technology*, vol. 34, no. 9, pp. 1455–1466, 2018.

[35] G. Zhang, L. Wu, A. Tang et al., "Growth behavior of MgAl-layered double hydroxide films by conversion of anodic films on magnesium alloy AZ31 and their corrosion protection," *Applied Surface Science*, vol. 456, pp. 419–429, 2018.

[36] G. Zhang, L. Wu, A. Tang et al., "Sealing of anodized magnesium alloy AZ31 with MgAl layered double hydroxides layers," *RSC Advances*, vol. 8, no. 5, pp. 2248–2259, 2018.

[37] H. Hirahara, S. Aisawa, T. Akiyama et al., "Intercalation of polyhydric alcohols into Mg–Al layered double hydroxide by calcination-rehydration reaction," *Clay Sci*, vol. 13, pp. 27–34, 2005.

[38] J.-Y. Uan, J.-K. Lin, and Y.-S. Tung, "Direct growth of oriented Mg-Al layered double hydroxide film on Mg alloy in aqueous HCO_3^-/CO_3^{2-} solution," *Journal of Materials Chemistry*, vol. 20, no. 4, pp. 761–766, 2010.

[39] J. K. Lin, C. L. Hsia, and J. Y. Uan, "Characterization of Mg,Al-hydrotalcite conversion film on Mg alloy and Cl- and CO32 - anion-exchangeability of the film in a corrosive environment," *Scripta Materialia*, vol. 56, no. 11, pp. 927–930, 2007.

[40] J.-Y. Uan, J.-K. Lin, Y.-S. Sun, W.-E. Yang, L.-K. Chen, and H.-H. Huang, "Surface coatings for improving the corrosion resistance and cell adhesion of AZ91D magnesium alloy through environmentally clean methods," *Thin Solid Films*, vol. 518, no. 24, pp. 7563–7567, 2010.

[41] J. K. Lin and J. Y. Uan, "Formation of Mg,Al-hydrotalcite conversion coating on Mg alloy in aqueous HCO3-/CO32- and

corresponding protection against corrosion by the coating," *Corrosion Science*, vol. 51, no. 5, pp. 1181–1188, 2009.

[42] B. Yu, J. Lin, and J. Uan, "Applications of carbonic acid solution for developing conversion coatings on Mg alloy," *Transactions of Nonferrous Metals Society of China*, vol. 20, no. 7, pp. 1331–1339, 2010.

[43] J.-K. Lin, K.-L. Jeng, and J.-Y. Uan, "Crystallization of a chemical conversion layer that forms on AZ91D magnesium alloy in carbonic acid," *Corrosion Science*, vol. 53, no. 11, pp. 3832–3839, 2011.

[44] J. Chen, Y. Song, D. Shan, and E.-H. Han, "In situ growth of Mg-Al hydrotalcite conversion film on AZ31 magnesium alloy," *Corrosion Science*, vol. 53, no. 10, pp. 3281–3288, 2011.

[45] J. Chen, Y. Song, D. Shan, and E.-H. Han, "Study of the in situ growth mechanism of Mg-Al hydrotalcite conversion film on AZ31 magnesium alloy," *Corrosion Science*, vol. 63, pp. 148–158, 2012.

[46] J. Chen, Y. Song, D. Shan, and E.-H. Han, "Study of the corrosion mechanism of the in situ grown Mg-Al-CO 32- hydrotalcite film on AZ31 alloy," *Corrosion Science*, vol. 65, pp. 268–277, 2012.

[47] J.-H. Syu, J.-Y. Uan, M.-C. Lin, and Z.-Y. Lin, "Optically transparent Li-Al-CO3 layered double hydroxide thin films on an AZ31 Mg alloy formed by electrochemical deposition and their corrosion resistance in a dilute chloride environment," *Corrosion Science*, vol. 68, pp. 238–248, 2013.

[48] F. Zhang, Z.-G. Liu, R.-C. Zeng et al., "Corrosion resistance of Mg-Al-LDH coating on magnesium alloy AZ31," *Surface and Coatings Technology*, vol. 258, pp. 1152–1158, 2014.

[49] L. Wang, K. Zhang, H. He, W. Sun, Q. Zong, and G. Liu, "Enhanced corrosion resistance of MgAl hydrotalcite conversion coating on aluminum by chemical conversion treatment," *Surface and Coatings Technology*, vol. 235, pp. 484–488, 2013.

[50] G. L. Song, "Corrosion behavior of magnesium alloys and protection techniques," *Surf. Eng. Light Alloys*, pp. 3–39, 2010.

[51] S. Thomas, N. V. Medhekar, G. S. Frankel, and N. Birbilis, "Corrosion mechanism and hydrogen evolution on Mg," *Current Opinion in Solid State & Materials Science*, vol. 19, no. 2, pp. 85–94, 2015.

[52] D. Song, A. B. Ma, J. H. Jiang, P. H. Lin, D. H. Yang, and J. F. Fan, "Corrosion behaviour of bulk ultra-fine grained AZ91D magnesium alloy fabricated by equal-channel angular pressing," *Corrosion Science*, vol. 53, no. 1, pp. 362–373, 2011.